JSES International 8 (2024) 646–653

Contents lists available at ScienceDirect

JSES International

journal homepage: www.jsesinternational.org

Three-dimensional corrective osteotomy for cubitus varus deformity using patient-matched instruments

Kunihiro Oka, MD[a,*], Satoshi Miyamura, MD[b], Ryoya Shiode, MD[b], Arisa Kazui, MD[b], Toru Iwahashi, MD[b], Hiroyuki Tanaka, MD[b], Tsuyoshi Murase, MD[c]

[a]Department of Orthopaedic Biomaterial Science, Graduate School of Medicine, Osaka University, Suita, Osaka, Japan
[b]Department of Orthopaedic Surgery, Graduate School of Medicine, Osaka University, Suita, Osaka, Japan
[c]Department of Orthopaedic Surgery, Bellland General Hospital, Sakai, Osaka, Japan

ARTICLE INFO

Keywords:
Computer simulation
Corrective osteotomy
Cubitus varus deformity
Surgical guide
Three-dimensional printing technology
Patient-matched instrument

Level of evidence: Level IV; Case Report; Treatment Study

Background: Various methods of two or three-dimensional (3D) corrective osteotomy for cubitus varus deformity have been reported. However, whether 3D correction of cubitus varus deformity is necessary is controversial because of technical difficulties and surgical complications. This study introduced 3D simulations and printing technology for corrective osteotomy against cubitus varus deformities. Moreover, recent studies on the application of these technologies were reviewed.
Methods: The amount of 3D deformity was calculated based on the difference in 3D shape between the affected side and the contralateral normal side. Patient-matched instruments were created to perform the actual surgery as simulated. Further, a 3D corrective osteotomy was performed using patient-matched instruments for cubitus varus deformity in pediatric and adolescent patients. The humerus-elbow-wrist angle, tilting angle, and elbow ranges of motion were evaluated.
Results: Humerus-elbow-wrist angle and tilting angle were corrected from −21° to 14° and from 30° to 43°, respectively, in the pediatric patient and from −18° to 10° and from 20° to 40°, respectively, in the adolescent patient. The elbow flexion and extension angles changed from 130° to 140° and from 20° to 10°, respectively, in the pediatric patient and from 120° to 130° and from 15° to 0°, respectively, in the adolescent patient.
Conclusion: The 3D computer simulations and the use of patient-matched instruments for cubitus varus deformity are reliable and can facilitate an accurate and safe correction. These technologies can simplify the complexity of 3D surgical procedures and contribute to the standardization of treatment for cubitus varus deformity.

Supracondylar fractures of the humerus are common injuries in children and account for approximately 60% of elbow fractures in children.[22,50] Cubitus varus deformities after supracondylar fractures are the most frequent complications. Its incidence ranges from 10% to 57%, regardless of the initial treatment.[10,12,30,37] Although the main complaint is often a cosmetic problem, various complications, including restriction of elbow flexion,[6,8,38] secondary fractures of the lateral condylar,[9,43] elbow instability and pain,[4,28] tardy ulnar palsy,[17,25,29] and degenerative change of the elbow joint[16,26] have been reported in the early, middle, and late stages due to changes in elbow joint alignment. To improve the appearance of the upper extremity to a symmetrical shape with a normal side and prevent late complications, various methods of corrective osteotomy have been reported. Traditionally, simple lateral closing-wedge osteotomy[12,16,49] and step-cut osteotomy[2,8,11] to reduce the lateral prominence, which corrects the coronal deformity with or without correction of the sagittal deformity, have been widely used because of their technical simplicity. However, cubitus varus deformities include extension and internal rotation deformities.[13,23,44,47] A multiplanar osteotomy to correct a three-dimensional (3D) deformity has also been advocated.[7,47] However, whether 3D correction is necessary for the correction of a cubitus varus deformity is controversial because of its technical difficulty and surgical complication.[3,34,41,42,51] Recent advances in

This study was approved by the Institutional Review Board of the Academic Clinical Research Center of Osaka University (approval no. 14179-2) and followed the tenets of the Declaration of Helsinki as revised in 2000. Each author certifies that their institution approved the human protocol for this investigation, all investigations were conducted in conformity with ethical principles of research, and informed consent was obtained from all study participants.

*Corresponding author: Kunihiro Oka, MD, Department of Orthopaedic Biomaterial Science, Graduate School of Medicine, Osaka University, 2-2, Yamada-oka, Suita, Osaka 565-0871, Japan.
E-mail address: okakunihiro@gmail.com (K. Oka).

https://doi.org/10.1016/j.jseint.2024.01.005
2666-6383/

computer simulation technology and patient-matched surgical guides and implants created by 3D printing technology have solved these problems and enabled accurate, simple, and safe 3D correction.[18,27,33,45,52] Thus, this study introduces 3D preoperative simulations and printing technology for corrective osteotomy of cubitus varus deformities and reviews recent studies on the application of these technologies.

Pathology of cubitus varus deformity

A cubitus varus deformity is a 3D deformity that includes extension and internal rotation in addition to the varus deformity.[3,23,47,52] The 3D analysis of 30 cases of cubitus varus deformity using 3D bone models showed that 44% had varus, extension, and rotation deformities; 20% had varus and extension deformities; 16% had varus and rotational deformities[44]; and 20% had varus deformity alone. As the mechanical axis of the elbow translates medially due to the varus deformity, axial stress is concentrated on the medial side of the elbow joint while the distraction force is generated on the lateral side, causing elbow joint instability due to lateral collateral ligament insufficiency.[4,28] The additional shear force causes secondary fractures of the lateral condylar.[9,43] The concentration of mechanical stress on the medial joint leads to a degenerative change in the elbow joint.[26] The extension deformity of the distal humerus reduces the anterior tilt of the condyles, and the offset of the elbow flexion and extension axis from the humeral longitudinal axis decreases. This reduces the space for the soft tissue between the upper arm and forearm at elbow flexion, limiting flexion motion beyond the angle of extension deformity.[20,35] The internal rotation deformity presents hyper-internal rotation and limited external rotation of the shoulder. As activities of daily living such as touching the ipsilateral ear, putting on a necklace, washing the face, and combing hair require shoulder external rotation of $\geq 60^{\circ}$, the rotational deformity should be corrected to at least $\leq 30^{\circ}$.[1,45] Rotational deformity also affects sports activities, including swimming and those involving throwing a ball or swinging and hitting a ball.

Extension deformities may be remodeled along the joint plane of motion until the age of 10; however, the distal humerus has little ability to spontaneously correct varus and internal rotation deformities.[5,15,42,48] Therefore, 3D correction for a cubitus varus deformity is recommended.

Preoperative simulation of 3D-corrective osteotomy

This study was approved by the institutional review board of Osaka University Hospital, Suita, Japan (approval number: 14179-2) and followed the tenets of the Declaration of Helsinki (as revised in 2000). Each author certifies that his or her institution approved the human protocol for this investigation, all investigations were conducted in conformity with the ethical principles of research, and informed consent was obtained from all study participants.

Evaluation of 3D deformity

Bilateral upper extremities, including the whole humerus and forearm bones, underwent computed tomography (CT) with a low-radiation protocol (scan pitch, 0.562:1; speed, 5.62 mm/rot, 30 mA, 120 kV), which reduced the radiation exposure from 1/10 to 1/5 compared with the normal setting.[31] 3D computer-generated bone models of bilateral humerus and forearm bones are created from CT data. The proximal part of the affected humerus is superimposed onto the corresponding part of the mirror image of the contralateral normal humerus, and the same procedure was applied to the distal part. This transformation of the affected humerus from the proximal superposition to the distal superposition is equivalent to the amount of 3D correction and the reverse of which indicates 3D deformity. The software automatically calculates the 3D deformity axis, which corresponds to the center of rotation of angulation of Paley's principle[36] adding translational deformity (Fig. 1, *A* and *B*). If the affected humerus is challenging to compare with the mirror image of the contralateral normal one due to severe joint deformity, the position of the forearm bones is used to determine the extent of correction with reference to the alignment of the upper extremity.

Planning 3D-corrective osteotomy

The distal osteotomy plane, created parallel to the joint line, is placed proximal to the olecranon fossa and near the 3D deformity axis. The location of the proximal osteotomy plane is determined by moving the distal osteotomy plane with the correction amount. After the removal of the wedge-shaped bone, which has a correction angle in the coronal and sagittal planes, the distal fragment was moved with the amount of correction. Then, the distal fragment was translated to the medial so that it aligned with the lateral cortex line, preventing lateral protrusion. Finally, the correction was completed with an adjustment of the rotation to obtain sufficient contact area of the distal and proximal fragments for stable fixation (Fig. 2, *A* and *B*).

Design of patient-matched surgical guides and plates

Patient-matched surgical guides and plates are created to enable clinicians to perform the actual surgery as preoperatively simulated. The surgical guide is embodied in rapid prototyping technology. The surgical guide is shaped to fit the posterolateral surface of the distal humerus and has osteotomy slits and four pipes for two sets of Kirschner wires at an angle to the deformity, and the configuration of the correction is achieved when they become parallel to each other, which are held with the reduction guide. After bone maturity in adolescence or adult cases, pipes are used to make predrilled holes for the patient-matched plate instead of Kirschner wire insertion. The patient-matched plate is designed to fit the bone surface after the correction (Fig. 3, *A-F*).

Surgical technique

A longitudinal posterior approach is used with the patient in the lateral decubitus position and the affected arm up. The medial side is exposed over the triceps fascia, and the ulnar nerve is released to protect it during surgery. The posterolateral surface of the distal humerus is exposed by the elevation of the lateral head of the triceps. The surgical guide is closely fitted to the bone surface, and the placement is confirmed by inserting a reference Kirschner wire penetrating the medial epicondyle (Fig. 4, *A*). Kirschner wires are inserted through the pipes, and the wedge-shaped osteotomy is completed with a bone saw through the slits (Fig. 4, *B*). After the removal of the wedge of the bone, the Kirschner wires, when parallel to each other, lead to the corrective position (Fig. 4, *C* and *D*). The parallel position can be held with the reduction guide. Lateral protrusion of the distal humerus can be prevented by aligning the lateral bone cortex of the osteotomy surfaces during correction. The osteotomy surface of the distal fragments that protruded medially should be trimmed accordingly. Finally, the distal fragment is fixed with tension band wiring of the lateral side and medial pinning. When the patient-matched plate is used, correction and fixation are automatically achieved by employing the patient-matched plate and inserting screws into the predrilled holes.

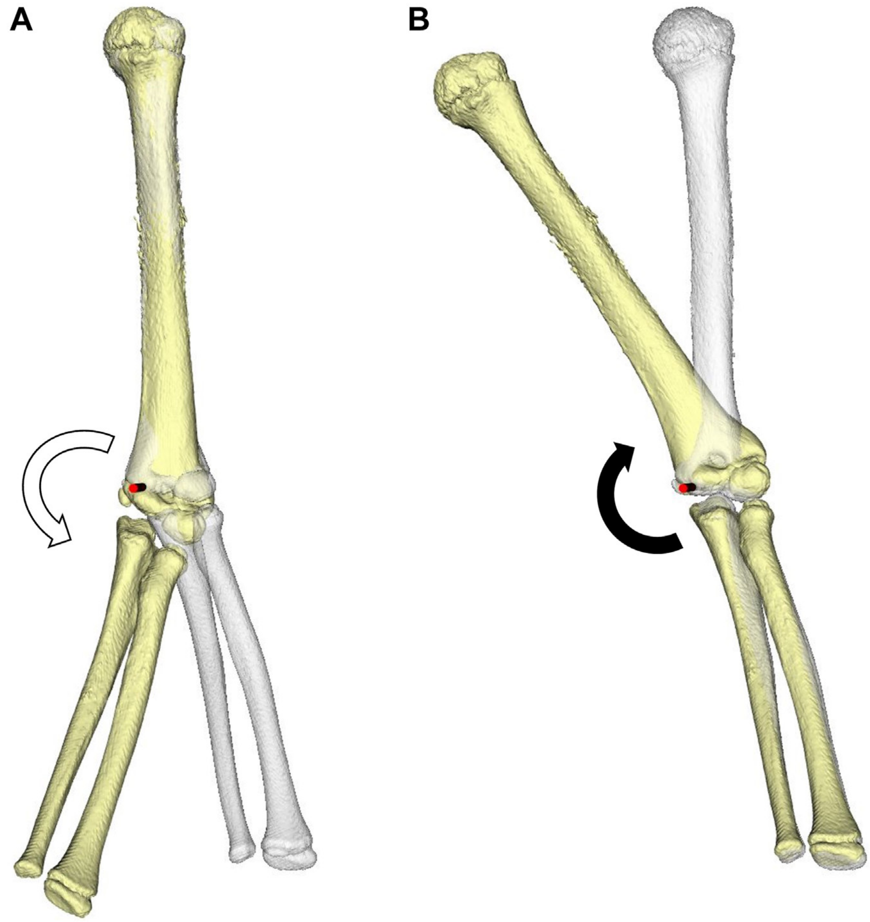

Figure 1 (**A**) Proximal and (**B**) distal superpositions between the affected humerus (*yellow*) and the mirror image of the contralateral normal humerus (*translucent gray*). The 3D correction angle (*white curved arrow*) around the deformity axis (*red axis*) could be calculated from the movement of the affected humerus from proximal to distal superposition. The reverse of the correction angle is the 3D deformity angle (*curved black arrow*). *3D*, three-dimensional.

In patients aged below 10 years, wherein osseous maturation remains incomplete, plates should be avoided to avert disruptions in growth and excessive invasion. Tension wiring fixation is implemented on the lateral side to prevent correction loss, concomitantly supplemented by medial pinning to forestall rotational displacement. In this age group, early bone union can be expected, and plate fixation is not required. As joint contractures are also unlikely to occur, active motion exercise of the elbow is initiated after immobilization with a cast for 3-4 weeks postoperatively. In patients aged >16 years who present with completed bone maturation, bilateral plates should be used to achieve long-term stabilization, ensure reliable bone union, and facilitate the early implementation of postoperative physical therapy. Adolescent patients require a greater fixation force compared with pediatric patients. Plate fixation is applied on the lateral side, and pinning or tension band wiring is added on the medial side to prevent rotation without impeding the axial diameter growth of the distal humerus. After the rest of the elbow is immobilized with a cast for 2 weeks, active motion exercise of the elbow is initiated.

Case presentation

Case 1

A 9-year-old boy sustained a supracondylar fracture of the left humerus when he was 4 years old (Video 1). He was treated with an immobilization cast, and the cubitus varus deformity remained. Then, the 3D evaluation of the deformity relative to the mirror image of the normal side revealed the following: 35° of varus, 15° of extension, and 10° of internal rotation deformity. The preoperative humerus-elbow-wrist angles (HEW-A) of the normal and affected sides were 14° and −21°, and the preoperative tilting angle (TA) of the normal and affected sides were 45° and 30°, respectively. After 3D corrective osteotomy, including rotational correction with a patient-matched surgical guide, HEW-A and TA were corrected to 14° and 43°, respectively (Fig. 5, *A* and *B*). The elbow flexion and extension angle changed from 130° to 140° and 20° to 10°, respectively.

Case 2

A 15-year-old boy sustained a supracondylar fracture of the left humerus at the age of 6 years. Although he was treated with closed reduction and percutaneous pinning, residual cubitus varus deformity remained. Next, 3D evaluation of the deformity relative to the mirror image of the normal side revealed the following: 30° of varus, 22° of extension, and 15° of internal rotation deformity. The preoperative HEW-A of the normal and affected sides were 12° and −18°, and the preoperative TA of the normal and affected sides were 42° and 20°, respectively. After 3D corrective osteotomy, including rotational correction with the patient-matched surgical guide and plate, HEW-A and TA were corrected to 10° and 40°, respectively (Fig. 6, *A*-*C*). The elbow flexion and extension angle changed from 120° to 130° and 15° to 0°, respectively.

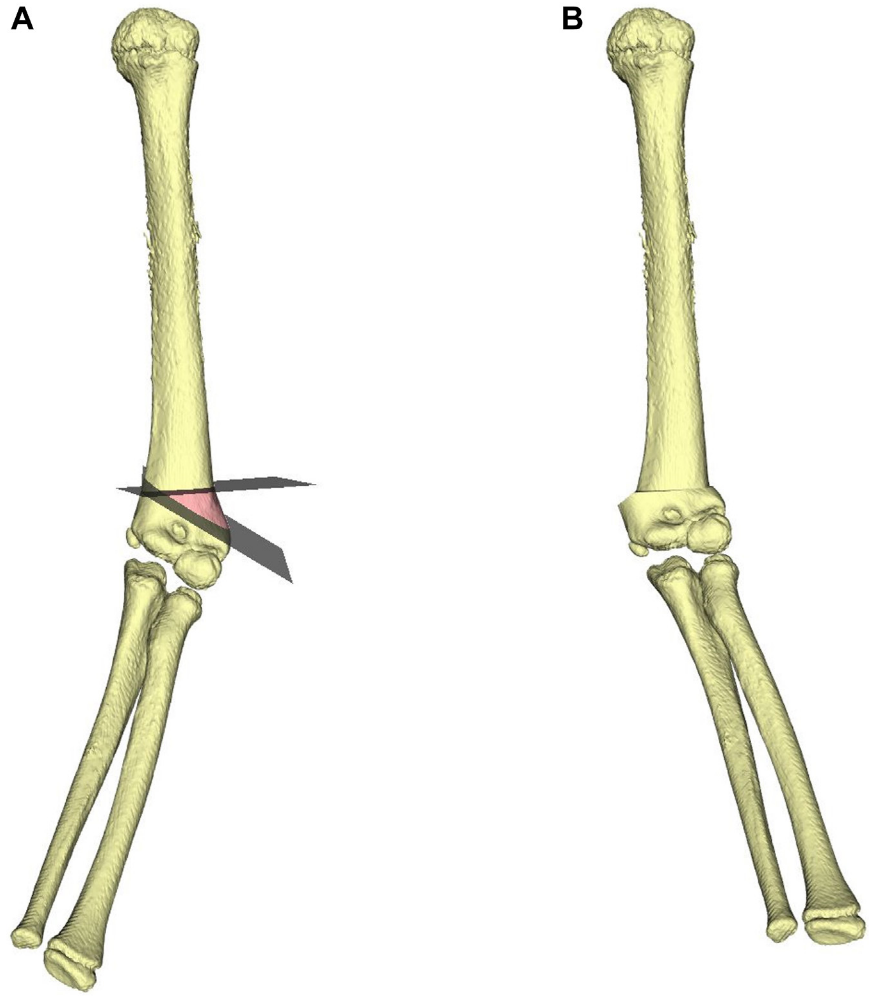

Figure 2 (**A**) Two osteotomy planes that have 3D correction angles are set on the distal humerus. (**B**) The correction is completed through fitting the osteotomy surfaces by aligning the lateral cortex and adjusting the rotation. *3D*, three-dimensional.

Utility of computer simulations and 3D surgical guides

Studies have reported corrective osteotomies for cubitus varus deformities using preoperative computer simulations and surgical guides, which emphasize their accuracy and utility. Jiang et al[18] reported corrective osteotomies based on preoperative computer simulations for 13 cubitus varus cases. The isosceles triangle of bone resection was planned on a computer, and Kirschner wires were used as a reference in the actual surgery. The mean varus of 20° was improved to the mean valgus of 11°, and the excellent and good rates were 92.3%. Takeyasu et al reported a 3D-corrective osteotomy using custom-made osteotomy templates for 30 cases of cubitus varus deformity. The mean difference in the HEW-A and TA between the affected and contralateral normal sides improved from 25.3° ± 7.0° to 1.3° ± 3.0° and from 14.9° to 1.9° ± 3.5°. The mean lateral prominence index improved from 9.1% ± 5.8% preoperatively to 4.8% ± 5.0% postoperatively. The mean internal rotational deformity decreased from 13.6° ± 11.2° preoperatively to 0.5° ± 2.1° postoperatively. The elbow range of motion returned to normal, with an increased flexion angle and decreased hyperextension. Moreover, 90% of the patients had excellent outcomes, and 10% had good outcomes. Oka et al analyzed five cases of cubitus varus deformities to verify the usefulness and safety of patient-matched surgical guides and plates for 12 cases of malunited fractures of the upper extremity.[33] The maximum deformity angle, which was calculated from the anteroposterior and lateral radiographs and indicated the true angular deformity, improved from 29.8° ± 3.5° to 3.0° ± 1.3°. In the evaluation of postoperative CT models, the average 3D correction errors compared with preoperative planning were <1.0° and <1.0 mm. Zhang et al[52] compared the surgical results of conventional corrective osteotomies with those of surgery assisted by 3D surgical guides. The operation time and blood loss were significantly shorter and less, respectively, in the 3D surgical guide group than in the conventional group. The rate of excellent deformity correction and excellent patient satisfaction were significantly higher in the 3D surgical guide group than in the conventional group. No significant differences in the postoperative carrying angle, elbow range of motion, or complications were found between the two groups. However, some negative reports were found regarding the usefulness of surgical guides for the corrective osteotomy of the cubitus varus deformity because of some reasons. No difference in treatment outcomes by other various surgical methods was found.[3,38] Good postoperative functional outcomes could be achieved by only the correction of the coronal plane, and 3D correction, including rotational deformity, has a risk of correction loss after surgery because of the reduction in the contact area of

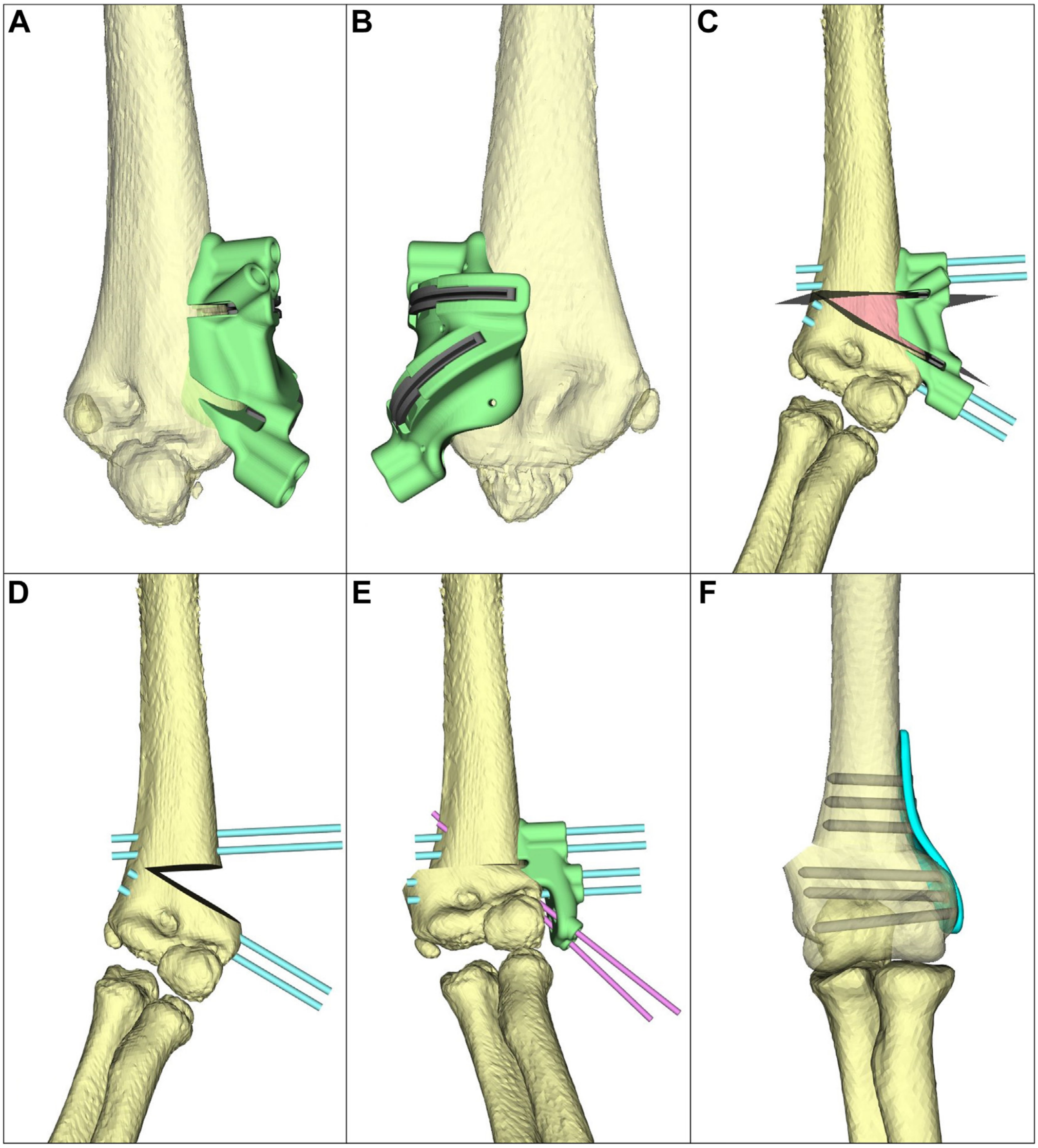

Figure 3 (**A**) Anterolateral (**B**) and posterior views of the patient-matched surgical guide (*green*) fit on the distal humerus (*translucent yellow*). (**C**) Two sets of Kirschner wires that had 3D correction angle are inserted through the pipes, and osteotomies are performed along the slits. (**D**) The wedge bone is removed with the patient-matched surgical guide. (**E**) The distal fragment is corrected by holding two sets of Kirschner wires (*blue*) parallel using the reduction guide, and two Kirschner wires (*pink*) are inserted from the distal pipes of the reduction guide for tension band wiring fixation. (**F**) In an adolescent whose epiphyseal line is closed, correction and fixation are completed simultaneously by placing the patient-matched plate and inserting the screws into a predrilled hole created by the guide. *3D*, three-dimensional.

the bone, which compromises fixation stability.[8,21,34,40,42] The creation of guides is expensive, the effectiveness of the surgery considering the time and financial costs of the creation of surgical guides is not considered high, and the additional radiation exposure from CT is a concern.[24,41,42] Nevertheless, the number of studies recommending 3D correction of cubitus varus deformity has been gradually increasing because of easier and familiar access to 3D computer simulations and rapid prototyping technology.[45,46,52] A 3D osteotomy using surgical guides enables correction into a symmetrical shape with the contralateral normal side without lateral protrusion, which may achieve high patient satisfaction.[14,45,52] The correction of 3D rotational deformity could recover the elbow motion, although residual rotational deformity would cause tardy ulnar palsy[17,25] and change elbow kinematics, leading to soft tissue and morphologic bony alterations in the elbow.[4,14,39] Radiation exposure could be reduced to a lower level than before because of low-dose imaging protocols and improved image processing programs. The wide use of patient-matched surgical guides in surgeries would reduce creation costs and the risk of revision surgery by reducing postoperative complications and lowering overall medical costs. The greatest advantage is that the surgery is highly reproducible and can minimize differences in surgeons' skills, contributing to the standardization of treatment.

Indications and disadvantages of corrective osteotomy with 3D surgical guides

Compared with conventional procedures, corrective osteotomy with 3D surgical guides occasionally requires a larger surgical field to place the surgical guide. It is essential to decrease the strip of periosteum to reduce the risk of late bone union or

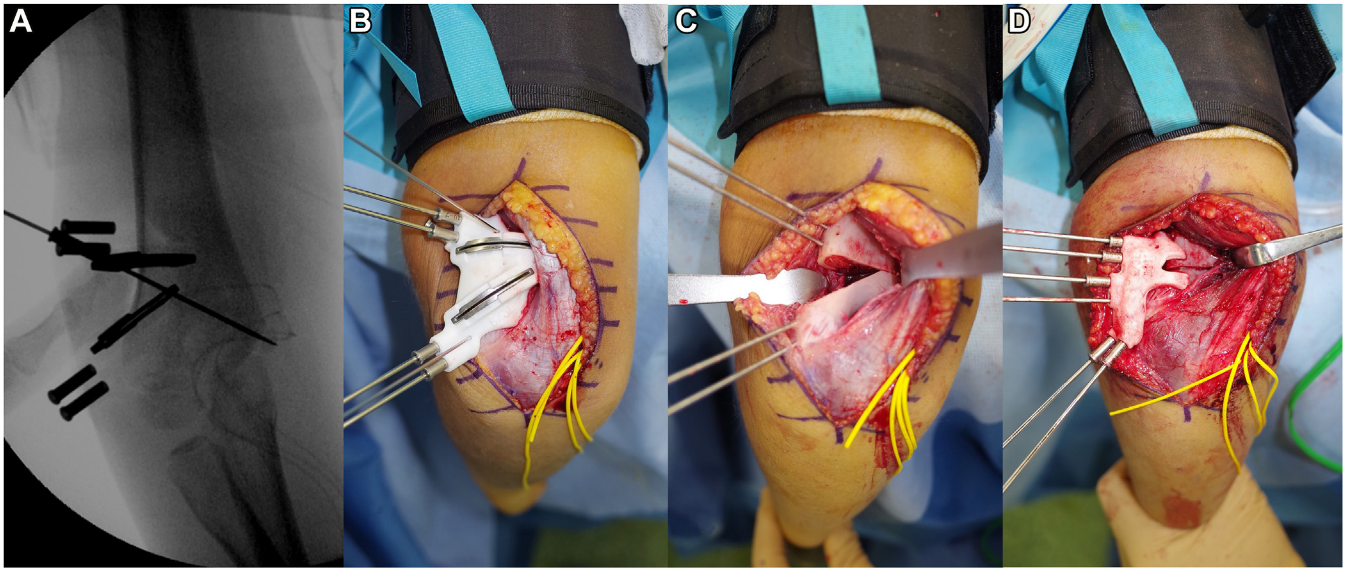

Figure 4 (**A**) The placement of the patient-matched guide is confirmed by the reference wire penetrating the tip of the medial condyle. (**B**) The patient-matched guide is fitted and fixed on the posterolateral bone surface. (**C**) After the osteotomy from the slits, the wedge-shaped bone is removed. (**D**) The cubitus varus deformity is corrected and fixed as planned using the reduction guide.

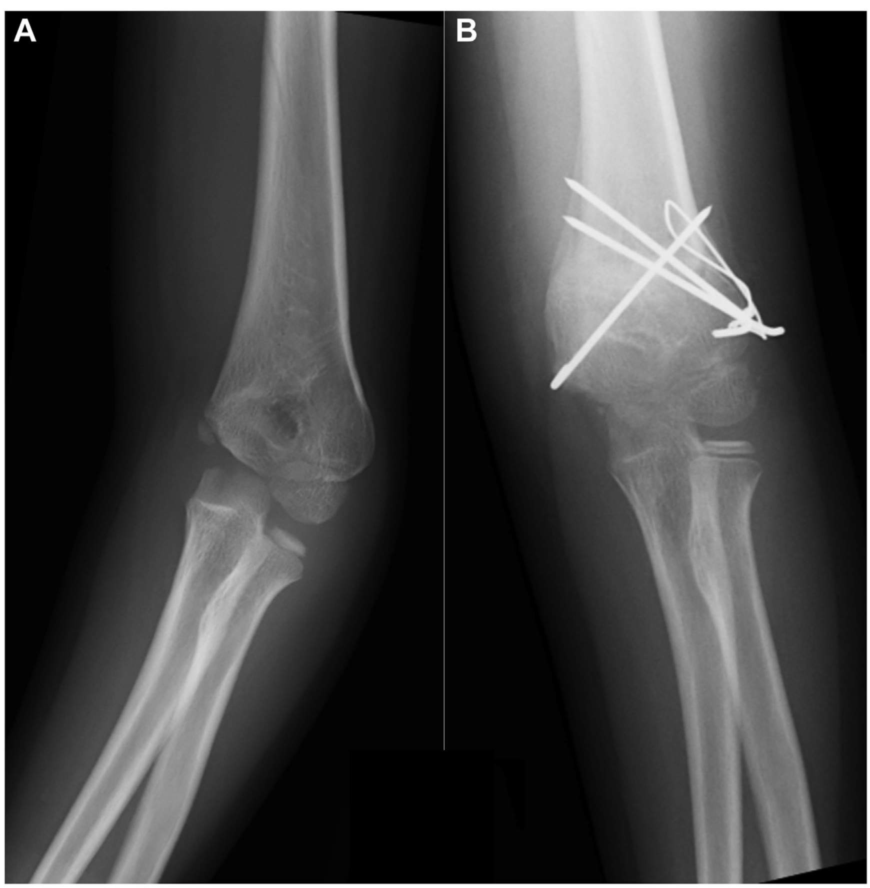

Figure 5 (**A**) Preoperative (**B**) and postoperative anteroposterior plain radiographs.

nonunion. Radial nerve injury, which can be caused by expanding the surgical field of the lateral humerus, should also be prevented. The 3D surgical guide must be placed on the dorsolateral safe zone of the distal humerus to prevent radial nerve injury. This area is located proximally along the lateral humeral shaft, from the lateral epicondyle to the level of the transepicondylar distance, where the radial nerve crosses the humerus in the midlateral plane.[19]

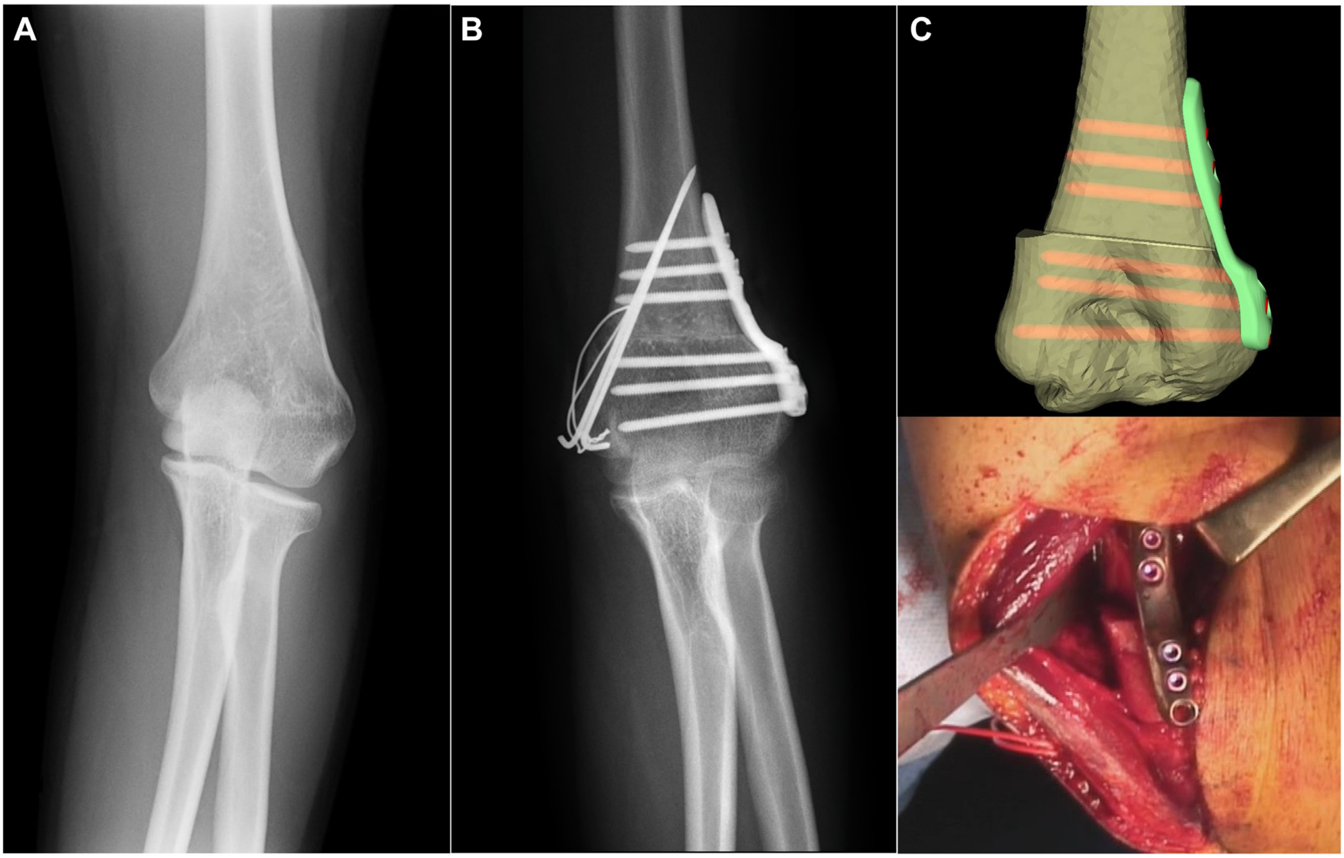

Figure 6 (**A**) Preoperative (**B**) and postoperative anteroposterior plain radiographs. (**C**) The upper part is the computer-aided design of the patient-matched plate, whereas the lower part is the intraoperative photograph of the patient-matched plate.

A larger varus deformity requires greater corrective angles, generally requiring more complicated surgery. One reason is that a large varus deformity can be challenging to fix after osteotomy because of an imbalance between the proximal and distal osteotomy surfaces. This imbalance can be eliminated by planning a corrective osteotomy of the partial lateral closing wedge and the partial medial opening wedge (Fig. 2, *A* and *B*). The ulnar nerve should be sufficiently released to prevent tension on it due to the lengthening of the medial side. Excessive correction of rotational deformity also results in an imbalance between the proximal and distal osteotomy surfaces. Considering the influence of fixating force and bone union, the extent of rotational correction should be adjusted to prevent leaving an internal rotation deformity of >30°, which could be a functional impairment.[1,45] In cases of severe deformity or the need for lengthening, which are challenging to correct with one-stage surgery, this procedure is contraindicated. Instead, correction via gradual lengthening with an external fixator or other procedures is recommended.

For intra-articular deformity, an intra-articular corrective osteotomy using 3D guides, as previously reported in cases of distal radius intra-articular malunion, can be performed. However, intra-articular osteotomies are associated with a potential risk of bone necrosis of the fragment or the development of osteoarthritic changes.[32] Especially, intra-articular osteotomies in children with an epiphyseal line that is not closed should be cautiously indicated. In cases of cubitus varus deformity after intra-articular fractures, such as varus deformity after lateral condyle fractures, if joint congruity is maintained, 3D extra-articular corrective osteotomy for correcting upper extremity alignment can prevent late complications due to cubitus varus deformity.

Conclusion

Preoperative 3D computer simulations and the use of patient-matched instruments in cubitus varus deformity are reliable and offer accurate and safe correction. These technologies can simplify the complexity of surgical 3D procedures and contribute to the standardization of the treatment of cubitus varus deformities. This technique has the potential to be the gold standard in the treatment of cubitus varus deformity in the future.

Disclaimers:

Funding: This work was supported by JSPS KAKENHI Grant No. JP 23K08612.
Conflicts of interest: Kunihiro Oka reports that he has received funding from the Japan Society for the Promotion of Science (JSPS) KAKENHI Grant No. JP 23K08612 for work related to the subject of this article. This source was involved in data collection, data analysis, and editing the manuscript. The other authors, their immediate families, and any research foundation with which they are affiliated have not received any financial payments or other benefits from any commercial entity related to the subject of this article.

Supplementary Data

Supplementary data to this article can be found online at https://doi.org/10.1016/j.jseint.2024.01.005.

References

1. Aizawa J, Masuda T, Koyama T, Nakamaru K, Isozaki K, Okawa A, et al. Three-dimensional motion of the upper extremity joints during various activities of daily living. J Biomech 2010;43:2915-22. https://doi.org/10.1016/j.jbiomech.2010.07.006.
2. Bali K, Sudesh P, Krishnan V, Sharma A, Manoharan SR, Mootha AK. Modified step-cut osteotomy for post-traumatic cubitus varus: our experience with 14 children. Orthop Traumatol Surg Res 2011;97:741-9. https://doi.org/10.1016/j.otsr.2011.05.010.
3. Bauer AS, Pham B, Lattanza LL. Surgical correction of cubitus varus. J Hand Surg Am 2016;41:447-52. https://doi.org/10.1016/j.jhsa.2015.12.019.
4. Beuerlein MJ, Reid JT, Schemitsch EH, McKee MD. Effect of distal humeral varus deformity on strain in the lateral ulnar collateral ligament and ulnohumeral joint stability. J Bone Joint Surg Am 2004;86:2235-42. https://doi.org/10.2106/00004623-200410000-00015.
5. Bukvić N, Kvesić A, Brekalo Z, Bosak A, Bukvić F, Karlo R. The problem of post-traumatic varization of the distal end of the humerus remaining after the recovery of a supracondylar fracture. J Pediatr Orthop B 2013;22:372-5. https://doi.org/10.1097/BPB.0b013e328360f8df.
6. Chess DG, Leahey JL, Hyndman JC. Cubitus varus: significant factors. J Pediatr Orthop 1994;14:190-2.
7. Chung MS, Baek GH. Three-dimensional corrective osteotomy for cubitus varus in adults. J Shoulder Elbow Surg 2003;12:472-5. https://doi.org/10.1016/s1058-2746(03)00090-9.
8. Davids JR, Lamoreaux DC, Brooker RC, Tanner SL, Westberry DE. Translation step-cut osteotomy for the treatment of posttraumatic cubitus varus. J Pediatr Orthop 2011;31:353-65. https://doi.org/10.1097/BPO.0b013e31821723a6.
9. Davids JR, Maguire MF, Mubarak SJ, Wenger DR. Lateral condylar fracture of the humerus following posttraumatic cubitus varus. J Pediatr Orthop 1994;14:466-70.
10. Davis RT, Gorczyca JT, Pugh K. Supracondylar humerus fractures in children. Comparison of operative treatment methods. Clin Orthop Relat Res 2000:49-55.
11. DeRosa GP, Graziano GP. A new osteotomy for cubitus varus. Clin Orthop Relat Res 1988:160-5.
12. Devnani AS. Late presentation of supracondylar fracture of the humerus in children. Clin Orthop Relat Res 2005:36-41. https://doi.org/10.1097/01.blo.0000152439.43810.11.
13. French PR. Varus deformity of the elbow following supracondylar fractures of the humerus in children. Lancet 1959;2:439-41.
14. Hu X, Zhong M, Lou Y, Xu P, Jiang B, Mao F, et al. Clinical application of individualized 3D-printed navigation template to children with cubitus varus deformity. J Orthop Surg Res 2020;15:111. https://doi.org/10.1186/s13018-020-01615-8.
15. Ippolito E, Caterini R, Scola E. Supracondylar fractures of the humerus in children. Analysis at maturity of fifty-three patients treated conservatively. J Bone Joint Surg Am 1986;68:333-44.
16. Ippolito E, Moneta MR, D'Arrigo C. Post-traumatic cubitus varus. Long-term follow-up of corrective supracondylar humeral osteotomy in children. J Bone Joint Surg Am 1990;72:757-65.
17. Jeon IH, Oh CW, Kyung HS, Park IH, Kim PT. Tardy ulnar nerve palsy in cubitus varus deformity associated with ulnar nerve dislocation in adults. J Shoulder Elbow Surg 2006;15:474-8. https://doi.org/10.1016/j.jse.2005.10.009.
18. Jiang H, Li M, Wu Y. Application of computer simulation in the treatment of traumatic cubitus varus deformity in children. Medicine (Baltimore) 2019;98:e13882. https://doi.org/10.1097/md.0000000000013882.
19. Kamineni S, Ankem H, Patten DK. Anatomic relationship of the radial nerve to the elbow joint: clinical implications of safe pin placement. Clin Anat 2009;22:684-8. https://doi.org/10.1002/ca.20831.
20. Kapandji AI. The elbow. In: Kapandji AI, editor. The physiology of the joints. London: Churchill Livingstone; 2007. p. 76-103.
21. Kumar R, Rangasamy K, Raj Gopinathan N, Sudesh P, Goni VG. Is modified reverse step-cut osteotomy better than Yun's reverse V osteotomy in paediatric cubitus varus deformity correction? A prospective, double-blinded, randomized controlled trial. Int Orthop 2022;46:2041-53. https://doi.org/10.1007/s00264-022-05429-7.
22. Landin LA. Fracture patterns in children. Analysis of 8,682 fractures with special reference to incidence, etiology and secular changes in a Swedish urban population 1950-1979. Acta Orthop Scand Suppl 1983;202:1-109.
23. Laupattarakasem W, Mahaisavariya B, Kowsuwon W, Saengnipanthkul S. Pentalateral osteotomy for cubitus varus. Clinical experiences of a new technique. J Bone Joint Surg Br 1989;71:667-70.
24. Li J, Wang J, Rai S, Ze R, Hong P, Wang S, et al. 3D-printed model and osteotomy template technique compared with conventional closing-wedge osteotomy in cubitus varus deformity. Sci Rep 2022;12:6762. https://doi.org/10.1038/s41598-022-10732-9.
25. Mitsunari A, Muneshige H, Ikuta Y, Murakami T. Internal rotation deformity and tardy ulnar nerve palsy after supracondylar humeral fracture. J Shoulder Elbow Surg 1995;4:23-9.
26. Miyamura S, Oka K, Abe S, Shigi A, Tanaka H, Sugamoto K, et al. Altered bone density and stress distribution patterns in long-standing cubitus varus deformity and their effect during early osteoarthritis of the elbow. Osteoarthritis Cartilage 2018;26:72-83. https://doi.org/10.1016/j.joca.2017.10.004.
27. Murase T, Takeyasu Y, Oka K, Kataoka T, Tanaka H, Yoshikawa H. Three-dimensional corrective osteotomy for cubitus varus deformity with use of custom-made surgical guides. JBJS Essent Surg Tech 2014;4:e6. https://doi.org/10.2106/jbjs.St.M.00044.
28. O'Driscoll SW, Spinner RJ, McKee MD, Kibler WB, Hastings H 2nd, Morrey BF, et al. Tardy posterolateral rotatory instability of the elbow due to cubitus varus. J Bone Joint Surg Am 2001;83:1358-69.
29. Ogino T, Minami A, Fukuda K. Tardy ulnar nerve palsy caused by cubitus varus deformity. J Hand Surg Br 1986;11:352-6.
30. O'Hara LJ, Barlow JW, Clarke NM. Displaced supracondylar fractures of the humerus in children. Audit changes practice. J Bone Joint Surg Br 2000;82:204-10.
31. Oka K, Murase T, Moritomo H, Goto A, Sugamoto K, Yoshikawa H. Accuracy analysis of three-dimensional bone surface models of the forearm constructed from multidetector computed tomography data. Int J Med Robot 2009;5:452-7. https://doi.org/10.1002/rcs.277.
32. Oka K, Shigi A, Tanaka H, Moritomo H, Arimitsu S, Murase T. Intra-articular corrective osteotomy for intra-articular malunion of distal radius fracture using three-dimensional surgical computer simulation and patient-matched instrument. J Orthop Sci 2009;22:684-8. https://doi.org/10.1016/j.jos.2019.11.005.
33. Oka K, Tanaka H, Okada K, Sahara W, Myoui A, Yamada T, et al. Three-dimensional corrective osteotomy for malunited fractures of the upper extremity using patient-matched instruments: a prospective, multicenter, open-label, single-arm trial. J Bone Joint Surg Am 2019;101:710-21. https://doi.org/10.2106/jbjs.18.00765.
34. Oppenheim WL, Clader TJ, Smith C, Bayer M. Supracondylar humeral osteotomy for traumatic childhood cubitus varus deformity. Clin Orthop Relat Res 1984:34-9.
35. Oura K, Shigi A, Oka K, Tanaka H, Murase T. Corrective osteotomy for hyperextended elbow with limited flexion due to supracondylar fracture malunion. J Shoulder Elbow Surg 2018;27:1357-65. https://doi.org/10.1016/j.jse.2018.03.026.
36. Paley D. Osteotomy concepts and frontal plane realignment. In: Principles of deformity correction. Berlin, Heidelberg: Springer Berlin Heidelberg; 2002. p. 99-154.
37. Piggot J, Graham HK, McCoy GF. Supracondylar fractures of the humerus in children. Treatment by straight lateral traction. J Bone Joint Surg Br 1986;68:577-83.
38. Solfelt DA, Hill BW, Anderson CP, Cole PA. Supracondylar osteotomy for the treatment of cubitus varus in children: a systematic review. Bone Joint J 2014;96-b:691-700. https://doi.org/10.1302/0301-620x.96b5.32296.
39. Spinner RJ, O'Driscoll SW, Davids JR, Goldner RD. Cubitus varus associated with dislocation of both the medial portion of the triceps and the ulnar nerve. J Hand Surg Am 1999;24:718-26.
40. Su Y, Nan G. Lateral closing isosceles triangular osteotomy for the treatment of a post-traumatic cubitus varus deformity in children. Bone Joint J 2016;98-b:1521-5. https://doi.org/10.1302/0301-620x.98b11.37890.
41. Su Y, Xie Y, Nan G. A novel method of lateral closing wedge osteotomy for cubitus varus deformity in children. BMC Surg 2022;22:408. https://doi.org/10.1186/s12893-022-01854-y.
42. Takagi T, Takayama S, Nakamura T, Horiuchi Y, Toyama Y, Ikegami H. Supracondylar osteotomy of the humerus to correct cubitus varus: do both internal rotation and extension deformities need to be corrected? J Bone Joint Surg Am 2010;92:1619-26. https://doi.org/10.2106/jbjs.I.00796.
43. Takahara M, Sasaki I, Kimura T, Kato H, Minami A, Ogino T. Second fracture of the distal humerus after varus malunion of a supracondylar fracture in children. J Bone Joint Surg Br 1998;80:791-7.
44. Takeyasu Y, Murase T, Miyake J, Oka K, Arimitsu S, Moritomo H, et al. Three-dimensional analysis of cubitus varus deformity after supracondylar fractures of the humerus. J Shoulder Elbow Surg 2011;20:440-8. https://doi.org/10.1016/j.jse.2010.11.020.
45. Takeyasu Y, Oka K, Miyake J, Kataoka T, Moritomo H, Murase T. Preoperative, computer simulation-based, three-dimensional corrective osteotomy for cubitus varus deformity with use of a custom-designed surgical device. J Bone Joint Surg Am 2013;95:e173. https://doi.org/10.2106/jbjs.L.01622.
46. Tanwar YS, Habib M, Jaiswal A, Singh S, Arya RK, Sinha S. Triple modified French osteotomy: a possible answer to cubitus varus deformity. A technical note. J Shoulder Elbow Surg 2014;23:1612-7. https://doi.org/10.1016/j.jse.2014.06.030.
47. Usui M, Ishii S, Miyano S, Narita H, Kura H. Three-dimensional corrective osteotomy for treatment of cubitus varus after supracondylar fracture of the humerus in children. J Shoulder Elbow Surg 1995;4:17-22.
48. Verka PS, Kejariwal U, Singh B. Management of cubitus varus deformity in children by closed dome osteotomy. J Clin Diagn Res 2017;11:Rc08-12. https://doi.org/10.7860/jcdr/2017/24345.9551.
49. Voss FR, Kasser JR, Trepman E, Simmons E Jr, Hall JE. Uniplanar supracondylar humeral osteotomy with preset Kirschner wires for posttraumatic cubitus varus. J Pediatr Orthop 1994;14:471-8.
50. Vu TN, Phung SHD, Vo LH, Nguyen UH. Diagnosis and treatment for pediatric supracondylar humerus fractures with brachial artery injuries. Children (Basel) 2021;8:933. https://doi.org/10.3390/children8100933.
51. You C, Zhou Y, Han J. A double-closed wedge broken-line osteotomy for cubitus varus deformity. Medicine (Baltimore) 2021;100:e26124. https://doi.org/10.1097/md.0000000000026124.
52. Zhang YW, Xiao X, Gao WC, Xiao Y, Zhang SL, Ni WY, et al. Efficacy evaluation of three-dimensional printing assisted osteotomy guide plate in accurate osteotomy of adolescent cubitus varus deformity. J Orthop Surg Res 2019;14:353. https://doi.org/10.1186/s13018-019-1403-7.